

Pavement condition assessment through jointly estimated road roughness and vehicle parameters

O.A. Shereena^a and B.N. Rao^{*}

Department of Civil Engineering, Indian Institute of Technology Madras, Chennai 600036, Tamil Nadu, India

(Received May 14, 2019, Revised October 1, 2019, Accepted October 4, 2019)

Abstract. Performance assessment of pavements proves useful, in terms of handling the ride quality, controlling the travel time of vehicles and adequate maintenance of pavements. Roughness profiles provide a good measure of the deteriorating condition of the pavement. For the accurate estimates of pavement roughness from dynamic vehicle responses, vehicle parameters should be known accurately. Information on vehicle parameters is uncertain, due to the wear and tear over time. Hence, condition monitoring of pavement requires the identification of pavement roughness along with vehicle parameters. The present study proposes a scheme which estimates the roughness profile of the pavement with the use of accurate estimates of vehicle parameters computed in parallel. Pavement model used in this study is a two-layer Euler–Bernoulli beam resting on a nonlinear Pasternak foundation. The asphalt topping of the pavement in the top layer is modeled as viscoelastic, and the base course bottom layer is modeled as elastic. The viscoelastic response of the top layer is modeled with the help of the Burgers model. The vehicle model considered in this study is a half car model, fitted with accelerometers at specified points. The identification of the coupled system of vehicle-pavement interaction employs a coupled scheme of an unbiased minimum variance estimator and an optimization scheme. The partitioning of observed noisy quantities to be used in the two schemes is investigated in detail before the analysis. The unbiased minimum variance estimator (MVE) make use of a linear state-space formulation including roughness, to overcome the linearization difficulties as in conventional nonlinear filters. MVE gives estimates for the unknown input and fed into the optimization scheme to yield estimates of vehicle parameters. The issue of ill-posedness of the problem is dealt with by introducing a regularization equivalent term in the objective function, specifically where a large number of parameters are to be estimated. Effect of different objective functions is also studied. The outcome of this research is an overall measure of pavement condition.

Keywords: pavement roughness; condition assessment; minimum variance estimator; optimization

1. Introduction

Pavement roughness indicates the presence of surface irregularities on the road profile and induces undesirable vibrations in the vehicles. Road profile excitation is regarded as one of the major sources of external disturbance in the road vehicle interaction dynamics. Gillespie and Sayers (1985) have shown that roughness contributes towards user discomfort and higher vehicle

^{*}Corresponding author, Professor, E-mail: bnrao@iitm.ac.in

^a Ph.D. Student, E-mail: shereena.oa@gmail.com

maintenance cost, and increases travel time due to speed reductions. Ride quality is a key indicator of pavement performance and significantly affects highway construction practice and maintenance, and pavement roughness directly influences ride quality (Alhasan *et al.* 2017). Pavement roughness provides a good, overall measure of pavement surface quality (Loizos 2001, Loizos and Plati 2002). Assessment of pavement condition is essential, in determining and designing for the ride quality. Road surface roughness influences roll stability, and handling stability is important for ride comfort and safety of the vehicle (Yang *et al.* 2015, Li *et al.* 2016). The maintenance of smooth road profiles also plays a major role in minimizing dynamic tire forces and promoting long pavement life spans (Gillespie *et al.* 1992, Green and Cebon 1994). The analysis and maintenance of a road surface is a difficult problem that pavement engineers have been facing for many years. Detection of the condition of a road profile is important for many other reasons as well, such as safety and economic savings.

Various techniques have been proposed to estimate road roughness profile, to assess the road serviceability condition. Earlier techniques of roughness measurement included the use of rod and level equipment or specialized dipstick walking profilometers. These techniques are slow and time consuming. The use of a laser sensor or ultrasonic sensor gives direct visualization of the profile, but the equipment is usually expensive, and data recorded may be highly noisy due to various factors (Sayers and Karamihas 1996, 1998). González *et al.* (2008) proposed the use of accelerometers fitted to the suspension system for the identification of road roughness, which is rather inexpensive. This work provides a road classification scheme based on a relationship between power spectral densities of vehicle accelerations rather than reconstructing a road profile. Harris *et al.* (2010) investigated the applicability of a combinatorial optimization technique for roughness estimation that makes use of vehicle vibration data and requires a calibrated vehicle model. Wei *et al.* (2015) developed a general regression neural network for identifying road roughness in the time domain based on vehicle angular acceleration data, which may not be practically easy to implement. Fauriat *et al.* (2016) proposed a data processing algorithm based on Kalman Filter for roughness identification. The estimation based on vehicle responses considers the roughness as a random walk process by combining the unknown roughness into the state vector, which results in suboptimal estimates. Alhasan *et al.* (2017) investigated the use of certain algorithms for processing laser scanning point clouds to obtain surface maps of roads. Haddar *et al.* (2018) introduced an algebraic estimator for road roughness estimation of different road classes. Data on vehicle parameters might be uncertain, and this uncertainty will lead to erroneous roughness estimates. On the other hand, the estimation of vehicle parameters from dynamic vehicle responses requires an accurate estimate of the roughness profile beforehand. This interrelationship points to the need for a joint estimation framework which simultaneously estimates vehicle parameters and roughness and filters the state measurements, to improve the accuracy of roughness estimates.

There are several vehicle parameter identification techniques. Hoshiya and Maruyama (1987) used a modified Extended Kalman Filter (EKF with Weighted Global Iteration) to identify the parameters of a moving load (SDOF) from beam response at a selected point and vehicle vibration data. Au *et al.* (2004) has applied a multi-stage optimization scheme based on genetic algorithms, modeling the vehicle as two degrees of freedom system, and using bridge response data. Chen and Lee (2008) used a Kalman filter along with an adaptive weighted recursive least square estimator to estimate the moving force on a bridge, while the vehicle-induced force was modeled as a sine wave. Lalthlamuana and Talukdar (2015) used a particle filter method to identify vehicle parameters from bridge acceleration measurements. The method does not require any calibration

process. However, the particle filter method assumes a pavement roughness measurement using a total station, which requires the closure of the bridge to obtain, thus limiting its applicability, especially for bridges that carry heavy traffic. Wang *et al.* (2017) have applied particle filtering to identify the vehicle parameters from bridge responses and estimated roughness, where the roughness is estimated beforehand using a probe car of calibrated parameters.

It is to be noted that direct profiling methods are usually expensive. Further, existing methods for roughness identification requires calibrated vehicle models. The roughness estimation (with known vehicle parameters) based on vehicle responses considers the roughness as a random walk process by combining the unknown roughness into the state vector, which results in suboptimal estimates (Fauriat *et al.* 2016). Also, estimating the vehicle parameters (for known roughness profile) by combining it in the state vector leads to nonlinear state-space equation and consequently suboptimal estimates due to linearization involved (Hoshiya and Maruyama 1987). An approach that incorporates the unknown inputs (roughness), as well as the system parameters in the state vector, constitutes a highly nonlinear state-space equation, which one needs to avoid. Apart from these, the recorded response data is always noisy. The present approach tries to overcome the above shortcomings by employing a linear state-space equation to avoid the need for any approximation in the form of linearization and by efficiently utilizing the observed data.

The current study proposes the coupling of an unbiased minimum variance estimator with an optimization scheme for the simultaneous estimation of vehicle parameters and road roughness. This study considers a half car vehicle model, instrumented to measure the vehicle vibration data. Recorded vibration data is partitioned into two sets. The first set of observation serves as the input for the unbiased minimum variance estimator (MVE) used for unknown input identification. The state estimates obtained from this step and corresponding to the second set of measurements is used for formulating an objective function that computes the error between the measured and computed dynamic responses. The objective function is minimized to obtain the vehicle parameters. The number of vehicle parameters to be estimated is varied in this study. Numerical investigations on the existence of a global minimum suggest that as the number of vehicle parameters to be estimated is increased, the objective function has to be modified by incorporating vehicle's natural frequency to ensure a well-posed problem. The effect of measurement noise on the estimation accuracy is investigated. Numerical results show that it is possible to accurately estimate the road roughness simultaneously in the presence of measurement noise, while vehicle parameters are estimated simultaneously.

2. Problem statement - condition of pavement from roughness estimates

Roughness is an indicator of deterioration of the pavement. Accurate estimation of roughness, in turn, requires good knowledge of the vehicle parameters. Parameters of vehicles in the experiment will not be known precisely and will not be the same as the design values, due to wear and tear with time. This aspect demands a simultaneous estimation of vehicle parameters and roughness, for accurate determination of roughness. Knowledge of the correct values of vehicle parameters and the road condition is essential also for the performance evaluation of vehicles on road or vehicle condition from the viewpoint of ride comfort. The entire estimation problem is formulated as an inverse problem and needs data in the form of vehicle acceleration measurements. The current formulation aims to employ minimum data which are conveniently measurable. Sensors are placed at selected points of the vehicle body and tires. In brief, this work attempts to

provide a condition measure through roughness estimated jointly with vehicle parameters for improved accuracy. Pavement model used, takes into account the viscoelastic nature. Effect of interaction between the pavement and vehicle is considered while simulating the response data.

3. Methodology - joint estimation framework of an optimization scheme and a minimum variance unbiased estimator

A combined scheme of an optimization technique and a minimum variance unbiased estimator (MVE) is employed to solve the problem of simultaneous estimation of roughness and vehicle parameters for providing a qualitative measure of pavement condition. Optimization scheme requires a set of initial conditions such as a specified range of vehicle parameters and a set of observation data. Minimization of the objective functions (Type 1 and Type 2) yields optimal sets of vehicle parameters and are then fed into the MVE. MVE, along with a second set of observed data input, yields roughness estimates. The detailed flow of the technique is depicted in the flowchart, illustrated in Fig. 1.

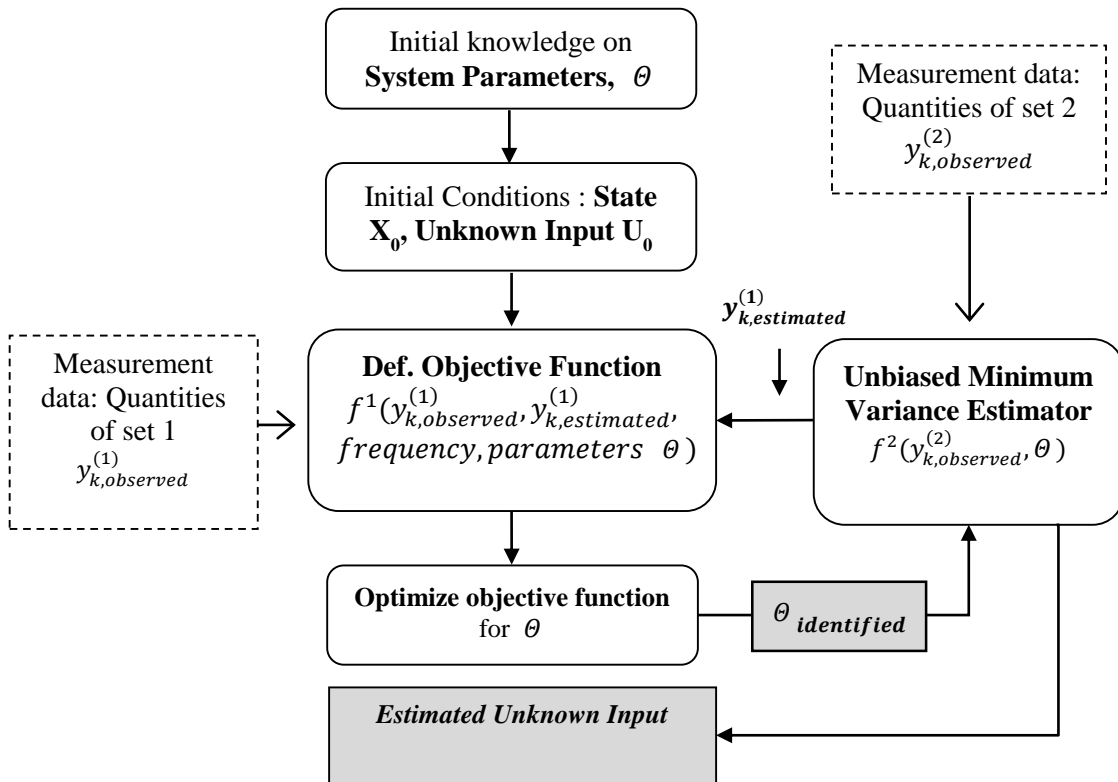


Fig. 1 Descriptive Flow chart of the proposed algorithm for joint estimation of unknown inputs and system parameters

The algorithm carries the combination of the two schemes in a coupled manner, giving out the estimates for vehicle parameters and roughness together. The partitioning of observation data into two schemes has to be investigated. The noisy data to be used in the optimization scheme is pre-filtered using a suitable filtering scheme for better performance. The vehicle-pavement system considered in this study uses a model which consists of a half car vehicle model on a pavement model of two-layer finite length Euler–Bernoulli beam with uniform cross-section resting on a nonlinear Pasternak foundation.

3.1 Half car model

The vehicle is represented by a half car model with negligible tire damping and four independent degrees of freedom, as shown in Figs. 2 and 5. The four degrees of freedom considered are the pitch and heave motions of the vehicle body (θ_v and y_v) and the vertical translation of the front and rear axles (y_1 and y_2). The vehicle body mass or sprung mass is represented by M_v and the axle components are represented by the unsprung masses m_1 and m_2 .

The sprung mass connects to the axle masses through a combination of springs of linear stiffness k_{s1} and k_{s2} , and viscous dampers with damping coefficients, C_{s1} and C_{s2} , which represent the suspension components for the front and rear axles. The axle masses then connect to the road surface through springs with linear stiffness, k_{t1} and k_{t2} , which represent the tire components for the front and rear axles.

The governing equations of a vehicle using half car model (Fig. 2) as given by Wu and Law (2011)

$$\begin{bmatrix} M_{v1} & 0 \\ 0 & M_{v2} \end{bmatrix} \ddot{X} + \begin{bmatrix} C_{v11} & C_{v12} \\ C_{v21} & C_{v22} \end{bmatrix} \dot{X} + \begin{bmatrix} K_{v11} & K_{v12} \\ K_{v21} & K_{v22} \end{bmatrix} X = - \begin{bmatrix} 0 \\ P(t) \end{bmatrix} + \begin{bmatrix} 0 \\ P_0 \end{bmatrix} \quad (1)$$

where the sub-matrices M_{v1} , M_{v2} , C_{v11} , C_{v12} , C_{v21} , C_{v22} , K_{v11} , K_{v12} , K_{v21} , and K_{v22} are given in Appendix B, $X = [x_v \ \theta_v \ x_{w1} \ x_{w2}]^T$. P_0 is the static load vector of the vehicle.

The interaction force vector is $P(t) = [P_1(t) \ P_2(t)]^T$ given by

$$\begin{aligned} P_1(t) &= (m_1 + a_2 m_v)g + k_{t1}(x_{w1} - w(\hat{x}_1(t), t) - r(\hat{x}_1(t))) \\ P_2(t) &= (m_2 + a_1 m_v)g + k_{t2}(x_{w2} - w(\hat{x}_2(t), t) - r(\hat{x}_2(t))) \end{aligned} \quad (2)$$

where $w(\hat{x}_1(t), t)$ and $w(\hat{x}_2(t), t)$ represents the displacement of the bridge under the front and rear wheel respectively, at the given time instant.

For half car model, the state X consists of vertical vehicle displacements and velocities. The parameters are shown in Fig. 2. The unknown input vector is the discrete point roughness at the rear and front wheel points. Thus the state vector X and unknown input u^* are given by

$$\begin{aligned} x &= [\dot{x}_v \ \dot{\theta}_v \ \dot{x}_{w1} \ \dot{x}_{w2} \ x_v \ \theta_v \ x_{w1} \ x_{w2}]^T \\ u^* &= [x_{r1} + w(\hat{x}_1(t), t) \ x_{r2} + w(\hat{x}_2(t), t)]^T \end{aligned} \quad (3)$$

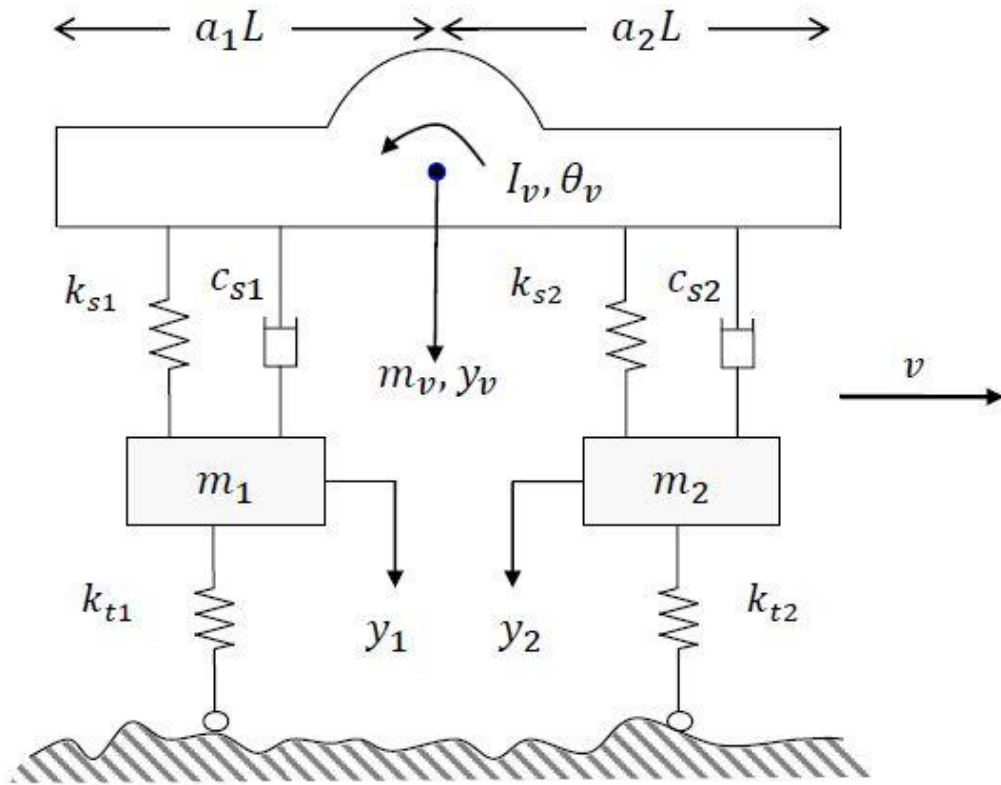


Fig. 2 Half Car Model

where x_{r1} and x_{r2} represents the roughness profile under the front and rear wheel respectively, based on the equation of motion for half car model Law *et al.* (2004), the matrix A_c and the vector G_c^* are provided in Appendix A.

The elements of measurement vector y_k to be used in MVE, as chosen based on the extensive analysis of different combinations in the forthcoming section 4.2, are vehicle accelerations and wheel displacements.

$$y_k = [\ddot{x}_v \quad \ddot{\theta}_v \quad \ddot{x}_{w1} \quad \ddot{x}_{w2} \quad x_{w1} \quad x_{w2}] \quad (4)$$

The terms C_k and H_k^* for half car model are provided in Appendix A.

3.2 Pavement model

The pavement is modeled as a two-layer finite length Euler-Bernoulli beam with a uniform cross-section, resting on a nonlinear Pasternak foundation, as detailed in Snehasagar *et al.* (2019). The top layer of the pavement is modeled as a viscoelastic asphalt topping based on Burger’s model, to incorporate the viscoelastic effects. The bottom layer is modeled as an elastic material representing the base course. The cross-section of the pavement is shown in Fig. 3. h_1 and h_2 represent the depth of the top and bottom layers, respectively. h_0 represents the depth of the neutral axis, and B denotes the width of the beam. Based on Euler-Bernoulli beam theory, for the equilibrium of stress, the following equation can be established (Yang *et al.* 2010). $w(x;t)$ represents the vertical deflection of the pavement.

$$E_1 \frac{\partial^2 w}{\partial x^2} \int_{h_0-h_1}^{h_0} Bz dz + E_2 \frac{\partial^2 w}{\partial x^2} \int_{h_0-h_1-h_2}^{h_0-h_1} Bz dz = 0 \tag{5}$$

where E_1 is the stiffness modulus of the asphalt top layer modeled as Hooke's material obtained based on the dynamic modulus and phase angle test results. E_2 is the elastic modulus for the bottom layer. The position of the neutral axis can be obtained as

$$h_0 = \frac{E_1 h_1^2 + E_2 (2h_1 + h_2) h_2}{2E_1 h_1 + 2E_2 h_2} \tag{6}$$

Burger’s viscoelastic model used in this study is schematically represented in Fig. 4. EV_1 , EV_2 , η_1 and η_2 are the parameters in Burger’s model (Mejrlun *et al.* 2017). The elasticity in the form of springs and viscosity in the form of dashpots are also depicted in Fig. 4. The corresponding stress-strain relationship ($\sigma - \mathcal{E}$) is

$$\sigma + p_1 \dot{\sigma} + p_2 \ddot{\sigma} = q_1 \dot{\mathcal{E}} + q_2 \ddot{\mathcal{E}} \tag{7}$$

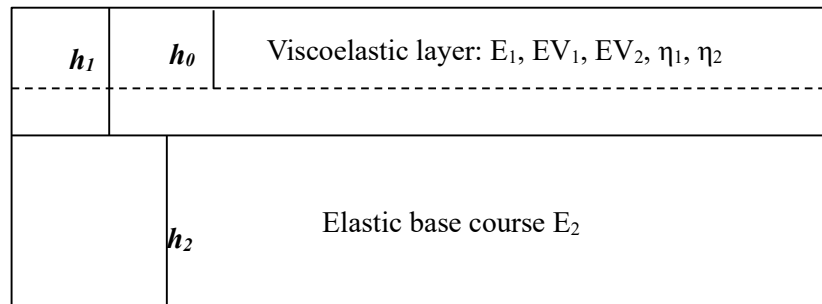


Fig. 3 Cross section of the pavement

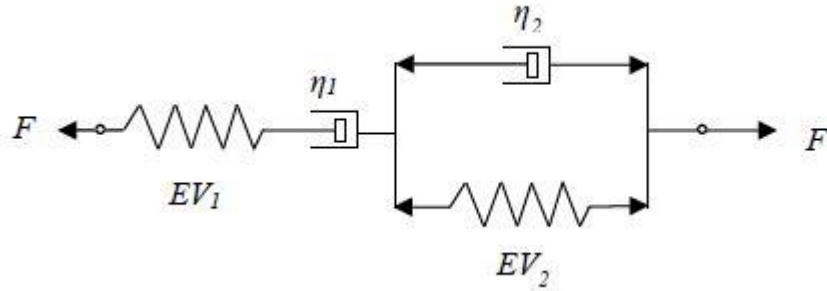


Fig. 4 The Burgers model

where

$$\begin{aligned}
 p_1 &= \frac{\eta_1 + \eta_2}{EV_2} + \frac{\eta_1}{EV_1}; & p_2 &= \frac{\eta_1\eta_2}{EV_1EV_2} \\
 q_1 &= \eta_1 & q_2 &= \frac{\eta_1\eta_2}{EV_2}
 \end{aligned}
 \tag{8}$$

The Relaxation modulus of the Burgers model is

$$E(t) = A_1 e^{-\alpha t} + B_1 e^{-\beta t}
 \tag{9}$$

where

$$\begin{aligned}
 \alpha &= \frac{p_1 + \sqrt{p_1^2 - 4p_2}}{2p_2} & \beta &= \frac{p_1 - \sqrt{p_1^2 - 4p_2}}{2p_2} \\
 A_1 &= \frac{\alpha q_2 - q_1}{\sqrt{p_1^2 - 4p_2}} & B_1 &= \frac{q_1 - \beta q_1}{\sqrt{p_1^2 - 4p_2}}
 \end{aligned}
 \tag{10}$$

The bending moment, M_x , in the pavement including the viscoelastic effects of the pavement top layer can be obtained as

$$M_x = - \int_{h_0-h_1}^{h_0} E_1 \frac{\partial^2 w}{\partial x^2} Bz^2 dz - \int_{h_0-h_1-h_2}^{h_0-h_1} E_2 \frac{\partial^2 w}{\partial x^2} Bz^2 dz - \int_{h_0-h_1}^{h_0} \int_0^t \dot{E}(t-\tau) d\tau \frac{\partial^2 w}{\partial x^2} Bz^2 dz
 \tag{11}$$

Integrating Eq. (11), the following equation can be obtained

$$M_x = -D_x \frac{\partial^2 w}{\partial x^2} - V_x \int_0^t \dot{E}(t-\tau) d\tau \frac{\partial^2 w}{\partial x^2} \tag{12}$$

where

$$D_x = \frac{E_1 B [h_0^3 - (h_0 - h_1)^3]}{3} + \frac{E_2 B [(h_0 - h_1)^3 - (h_0 - h_1 - h_2)^3]}{3} \tag{13}$$

$$V_x = \frac{B [h_0^3 - (h_0 - h_1)^3]}{3} \tag{14}$$

For the beam with density ρ , area of cross-section A and subjected to surface force $q(x; t)$, the following relationships are established through equilibrium equations

$$\frac{\partial M_x}{\partial x} - Q_x = 0, \quad \frac{\partial Q_x}{\partial x} - \rho A \frac{\partial^2 w}{\partial t^2} + q(x, t) = 0 \tag{15}$$

where Q_x represents the shear force. The equation of equilibrium can be finally simplified as

$$q(x, t) = \rho A \frac{\partial^2 w}{\partial t^2} + D_x \frac{\partial^4 w}{\partial x^4} + V_x \int_0^t \dot{E}(t-\tau) d\tau \frac{\partial^4 w}{\partial x^4} \tag{16}$$

The foundation is considered as a nonlinear Pasternak foundation with linear-plus-cubic stiffness, shear deformation, and viscous damping. The force induced by the foundation per unit length of the beam is given as

$$P = k_1 w + k_3 w^3 + \mu \frac{\partial w}{\partial t} - G_p \frac{\partial^2 w}{\partial x^2} \tag{17}$$

where k_1 , k_3 are the linear and nonlinear foundation parameters, respectively. G_p is the shear deformation coefficient and μ is the damping coefficient. Based on Eq. (2) for moving load P_i , the dynamic equation of the motion for the pavement Eq. (16) can be written as

$$\begin{aligned} & \rho A \frac{\partial^2 w}{\partial t^2} + D_x \frac{\partial^4 w}{\partial x^4} + V_x \int_0^t \dot{E}(t-\tau) d\tau \frac{\partial^4 w}{\partial x^4} + k_1 w + k_3 w^3 + \mu \frac{\partial w}{\partial t} - G_p \frac{\partial^2 w}{\partial x^2} \\ & = \sum_{i=1}^{N_p} P_i(t) \delta(x - v_i) \end{aligned} \tag{18}$$

N_p is the number of wheel contact points or size of the interaction force vector. $N_p = 2$ in case of half car model. All other symbols carry the same meaning as in the previous equations.

3.3 Modelling the vehicle-pavement interaction

The Galerkin method is employed to discretize the pavement differential equation (Eq. (18)). The series expansion for $w(x, t)$ is

$$w(x, t) = \sum_{k=1}^{\infty} q_k(t) \phi_k(x) \quad (19)$$

where $\phi_k(x)$ are the trial functions and $q_k(t)$ constitute the set of generalized displacements of the beam.

In this case, the first n terms are considered in the expansion in order to determine $w(x, t)$. The Eq.(18) is simplified using Eq. (19) based on the procedure outlined by Snehasagar *et al.* (2019). In Eq. (18), $P_i(t)$ represents the interaction force vector which is obtained by solving the vehicle dynamic equations (Eq. (1)). This coupling between the vehicle equations of motion and the pavement equation is realized through a decoupled iterative technique presented by Krishnanunni and Rao (2019). The method is based on solving the vehicle and pavement equations of motion separately and equating the interaction force at each time step. The solution goes through an iterative process in calculating the pavement displacement under the vehicle $w(x(t), t)$ until the increase in pavement displacement in two subsequent cycles is less than 1%. The main steps in the procedure are outlined below:

Step 1: Pavement displacement under the vehicle ($w(x(t), t)$) is assumed to be 0 initially for the entire simulation time.

Step 2: Vehicle responses are computed using Newmark's method based on Eq. (1).

Step 3: The computed vehicle responses are used to compute $P_i(t)$ based on Eq. (2).

Step 4: The pavement equations (Eq. (18)) are solved numerically to compute w from which ($w(x(t), t)$) (for both the front and rear wheel) can be computed for the entire simulation time.

Step 5: The procedure is repeated with the newly calculated ($w(x(t), t)$) until solution convergence is achieved.

The final vehicle responses obtained are used for the roughness identification so that the effect of vehicle-pavement interactions on the roughness estimation could be ascertained.

3.4 Data partitioning

The decision on how to partition the observed data between the two schemes is crucial for the success of the whole estimation process. There are mainly two criteria for partitioning. First, the observability criterion ($H_k \neq 0$) should be satisfied. Meeting the first constraint will filter out certain combinations. Second, the least square error should be minimum for the combination of data in MVE. Numerical investigations are carried out to find the best set of observation data for MVE or roughness estimation for a trial set of vehicle parameters. Based on the recognized set of observations that can be best utilized in MVE, the measurement data that can be utilized in the objective function may be chosen. Preferably, displacement quantities are used in the optimization scheme, as they are differentiable. Generally, in the field, accelerations are recorded, and other

vibration data may be deduced. In this study, data set I refer to the quantities that are fed into the MVE scheme, and set II for the data into the optimization scheme.

3.5 Minimum variance unbiased estimator

Minimum variance unbiased estimator used in this work has the structure of a Kalman filter and is designed for discrete linear systems with unknown inputs. This recursive filter performs joint estimation of states and inputs, where the states and inputs are interconnected (Gillijns and De Moor 2007). For the application of the filter, no prior knowledge regarding the unknown inputs is required. General description of the system is as follows

$$\begin{aligned} x_{k+1} &= A_k x_k + G_k d_k + w_k \\ y_k &= C_k x_k + H_k d_k + v_k \end{aligned} \quad (20)$$

$x_k \in R^n$ is the state vector. $d_k \in R^p$ is the unknown input vector and $y_k \in R^m$ the measurement vector and $w_k \in R^n$ and $v_k \in R^m$ are the process noise and the measurement noise respectively, uncorrelated white noises with mean zero and with covariance matrices $E[w_k w_k^T] = Q_k$ and $E[v_k v_k^T] = R_k$. The coefficient matrices A_k , G_k , C_k and H_k are assumed to be known. The rank of the matrix H_k is assumed to be equal to p , the size of the unknown input vector. The condition ($\text{rank } H_k = p$) is the necessary and sufficient condition for the unbiasedness of the estimator, and is critical in determining the observability of the system.

The summary of the filtering equations is given below (Gillijns and De Moor 2007)

Initialization

$$\hat{x}_0 = E[x_0] \quad (21)$$

$$P_0^x = E[(x_0 - \hat{x}_0)(x_0 - \hat{x}_0)^T] \quad (22)$$

Time update

$$\hat{x}_{k+1|k} = A_k \hat{x}_{k|k} + G_k \hat{d}_k \quad (23)$$

$$P_{k+1|k}^x = \begin{bmatrix} A_k & G_k \end{bmatrix} \begin{bmatrix} P_{k|k}^x & P_k^{xd} \\ P_k^{dx} & P_k^d \end{bmatrix} \begin{bmatrix} A_k^T \\ G_k^T \end{bmatrix} + Q_k \quad (24)$$

Estimation of unknown input

$$\tilde{R}_k = C_k P_{k|k-1}^x C_k^T + R_k \quad (25)$$

$$M_k = (H_k^T \tilde{R}_k^{-1} H_k)^{-1} H_k^T \tilde{R}_k^{-1} \quad (26)$$

$$\hat{d}_k = M_k (y_k - C_k \hat{x}_{k|k-1}) \quad (27)$$

$$P_k^d = (H_k^T \tilde{R}_k^{-1} H_k)^{-1} \quad (28)$$

Measurement update

$$K_k = P_{k|k-1}^x C_k^T \tilde{R}_k^{-1} \quad (29)$$

$$\hat{x}_{k|k} = \hat{x}_{k|k-1} + K_k (y_k - C_k \hat{x}_{k|k-1} - H_k \hat{d}_k) \quad (30)$$

$$P_{k|k}^x = P_{k|k-1}^x - K_k (\tilde{R}_k - H_k P_k^d H_k^T) K_k^T \quad (31)$$

$$P_k^{xd} = (P_k^{dx})^T = -K_k H_k P_k^d \quad (32)$$

3.6 Optimization scheme

Optimization scheme used in this work is the Cuckoo search algorithm (Yang and Deb 2009). In this study, two types of objective functions are used which are being described in the section below and as proposed by Krishnanunni *et al.* (2019). Any metaheuristic based optimization algorithms can be employed in the implementation of the proposed technique such as Particle Swarm Optimization scheme.

3.7 Objective functions

The objective function of type 1 minimizes the L2 norm of the selected set (based on data partitioning) of dynamic responses observed quantities. This approach works well for a minimum number of unknowns, where the optimization problem is still well-posed. As the number of unknown parameters increases, the problem becomes ill-posed. The need for regularisation of the objective function arises, and an additional information inclusion improves the situation. Thus, the objective function of type 2 consists of an additional term of extra information deduced from the observed data and knowledge about the system. Objective functions are structured as follows

Type 1

$$J_1 = \sum_{i=1}^{n_y} \sum_{j=1}^{n_t} (y_{ij}^{(1)} - \hat{y}_{ij}^{(1)})^2 \quad (33)$$

where n_y and n_t represent the number of set 2 quantities and number of time steps respectively.

Type 2

The objective function, in this case, contains an additional term based on frequency data. λ_k denotes the k^{th} mode frequency extracted from the measurement time history, applying the Fast Fourier Transform (FFT). $\hat{\lambda}_k$ computed for the k^{th} mode is a function of the vehicle parameter

values.

$$J_2 = \sum_{i=1}^{n_y} \sum_{j=1}^{n_r} (y_{ij}^{(1)} - \hat{y}_{ij}^{(1)})^2 + \sum_{k=1}^{n_{modes}} (\lambda_k - \hat{\lambda}_k)^2 \quad (34)$$

Frequencies estimated from the direct observations are found to be accurate under practical noise levels and efficient in providing good estimates.

4. Numerical illustration

Roughness estimation is carried out, using the simultaneous identification algorithm as detailed in section 3. In this study, pavement is modelled as a two-layer Euler-Bernoulli beam, with the top layer being viscoelastic for a most realistic scenario, and as resting on a nonlinear Pasternak foundation. The viscoelastic response of the top layer is obtained, considering Burger's model. Table 1 lists the physical and geometric properties of the pavement and the foundation. The foundation model (Snehasagar *et al.* 2019) used, has provided comparable deflection values with field measurements and hence adds to the level of accuracy in the current estimation procedure. Road roughness class A profile used in this study is generated in accordance with ISO 8608 (Agostinacchio *et al.* 2014), based on the power spectral density of road roughness. For the vehicle, the half car model is considered, and the parameter values are listed in Table 3 (Wu and Law 2011). The present study ignores the tire damping because the tire damping values are comparably small with respect to the vehicle damping values, and for mathematical simplicity. Using a discretization scheme, the system equations are solved to find the dynamic responses. It may be noted that the interaction dynamics is incorporated in the dynamic analysis. Then, equivalent actual field responses are generated by adding White Gaussian Noise according to Lyons (2004). Addition of white noise simulates synthetic data which is close to a practical scenario, in this work. Length of the stretch of road for observation generation is 140 meters. The roughness identification is carried out for the stretch (60-100) meters, as shown highlighted in Fig. 5. The initial conditions, i.e., the initial state values are set as the values calculated at the time point when the front wheel reaches 60.0 m, from the starting point. The calculations are carried out, considering a time step of 0.0005 s and vehicle velocity of 15 m/s. The proposed technique performs the simultaneous estimation of vehicle parameters and unknown input roughness, along with the estimation of response states. The scheme combines two existing techniques, in such a way that the estimates are optimal and unique. The formulation without the need of linearization, as exists in MVE paves the way for a set of optimal solutions. The employment of an idea of partitioning observations (Section 4.2) between the MVE and optimization scheme ensures unique solutions.

4.1 Initialization for MVE

The identification process is essentially an inverse problem, with the dynamic response data at hand. Initial conditions for the minimum variance estimator are to be specified. i.e., Considering an in-between stretch (60.00-100.0) m of the pavement of total length 140 m, initial velocities and displacements have to be specified, i.e., at 60 m from the starting point. Assumed to be known with quantified uncertainty. i.e., initial covariances for the use in MVE.

Table 1 Properties of the asphalt mixture, pavement, foundation and load (Ding *et al.* 2014, Mejlun *et al.* 2017)

Item	Notation	Value
Foundation		
Linear stiffness	k_1	$100 \times 10^6 \text{ N/m}^2$
Nonlinear stiffness	k_3	$100 \times 10^6 \text{ N/m}^2$
Viscous damping	μ	$0.3 \times 10^6 \text{ N s/m}^2$
Shear parameter	G_p	$6.66 \times 10^7 \text{ N}$
Beam properties		
Young's modulus of top layer	E_1	21,237 MPa
Young's modulus of bottom layer	E_2	400 MPa
Height of top layer	h_1	0.2 m
Height of bottom layer	h_2	0.2 m
Length of pavement	L	140 m
Width of pavement	B	1 m
Wavelength of road roughness	L_0	10 m
Amplitude of road roughness	l	0.0002 m

Table 2 Viscoelastic properties of the asphalt mixture at 20°C (Mejlun *et al.* 2017)

Notation	Value
EV_1	23,172 Mpa
EV_2	10,730 MPa
η_1	4,313 MPa.s
η_2	2,457 MPa.s

The initial covariance matrices used in this study, are given as follows

$$P_k = 10I_8, \quad P_k^d = 10I_2$$

where I denotes Identity matrix, with the subscript of its size.

$$Q_k = 0.1I_8, \quad R_k = 0.1I_{\text{no.of observations}}$$

With due consideration to the applicability of the technique in the field, the set of vehicle response quantities for data assimilation are selected based on the convenience of measuring at the field, as well. Numerical investigations are carried out to find the best partitioning scheme among the two schemes, as described in section 4.2. Initial conditions for MVE is given in section 4.1.

4.2 Partitioning the observation data

The best split of measurement data for a half car model, arrived and used in this study is $[\ddot{x}_v, \ddot{\theta}_v, \ddot{x}_{w1}, \ddot{x}_{w2}, x_{w1}, x_{w2}]$ in the MVE and $[x_v, x_\theta]$ in the objective function. To satisfy the observability criterion ($H_k^* \neq 0$), the wheel accelerations, $[x_{w1}, x_{w2}]$ is included in all the combinations tested. The combinations thus arrived, are then investigated numerically for choosing the best set for MVE, i.e. the set that maximizes the efficiency of the MVE. The results are summarized in Table 4. 10% noise is considered in the measurements. The vehicle parameters in Table 3 is considered for the study.

The error in estimation (E_r) in Table 4 is defined as

$$E_r = \frac{1}{mn} \sum_{j=1}^n \sqrt{\sum_{i=1}^m (x_{ri}^j - \hat{x}_{ri}^j)^2} \tag{35}$$

where m is the number of sampling points in the measurement and n is the number of independent noise-contaminated samples used. Here, $n = 100$ is adopted. Table 4 shows that the measurement combination MVE VI $[\ddot{x}_v, \ddot{x}_\theta, \ddot{x}_{w1}, \ddot{x}_{w2}, x_{w1}, x_{w2}]$ yields the least error in roughness estimation and hence, the most efficient. This finding recommends the partitioning such that the use of MVE VI combination in MVE scheme and the vehicle body displacements, $[x_v, x_\theta]$ in the objective function.

Table 3 Physical Constants of Half Car Model

Physical constants	Values
M_v	17735(kg)
I_v	1.47×10^5 (kg-m ²)
m_1	1500 (kg)
m_2	1000 (kg)
k_{s1}	2.47×10^6 (N-m)
c_{s1}	3.0×10^4 (N-s/m)
k_{s2}	4.23×10^6 (N-m)
c_{s2}	4.0×10^4 (N-s/m)
k_{t1}	3.74×10^5 (N-m)
k_{t2}	4.6×10^5 (N-m)

Table 4 Error (Er) in roughness identification considering different measurement combinations

MVE	Measurement Combination	Estimation error (E_r)
MVE I	$\ddot{x}_\theta, \ddot{x}_{w1}, \ddot{x}_{w2}$	2.74×10^{-4}
MVE II	$\ddot{x}_v, \ddot{x}_{w1}, \ddot{x}_{w2}$	2.20×10^{-4}
MVE III	$\ddot{x}_v, \ddot{x}_\theta, \ddot{x}_{w1}, \ddot{x}_{w2}$	1.26×10^{-4}
MVE IV	$\ddot{x}_v, \ddot{x}_\theta, \ddot{x}_{w1}, \ddot{x}_{w2}, x_{w1}$	1.22×10^{-4}
MVE V	$\ddot{x}_v, \ddot{x}_\theta, \ddot{x}_{w1}, \ddot{x}_{w2}, x_{w2}$	1.23×10^{-4}
MVE VI	$\ddot{x}_v, \ddot{x}_\theta, \ddot{x}_{w1}, \ddot{x}_{w2}, x_{w1}, x_{w2}$	1.17×10^{-5}

where m is the number of sampling points in the measurement and n is the number of independent noise-contaminated samples used. Here, $n = 100$ is adopted. Table 4 shows that the measurement combination MVE VI $[\ddot{x}_v, \ddot{x}_\theta, \ddot{x}_{w1}, \ddot{x}_{w2}, x_{w1}, x_{w2}]$ yields the least error in roughness estimation and hence, the most efficient. This finding recommends the partitioning such that the use of MVE VI combination in MVE scheme and the vehicle body displacements, $[x_v, x_\theta]$ in the objective function.

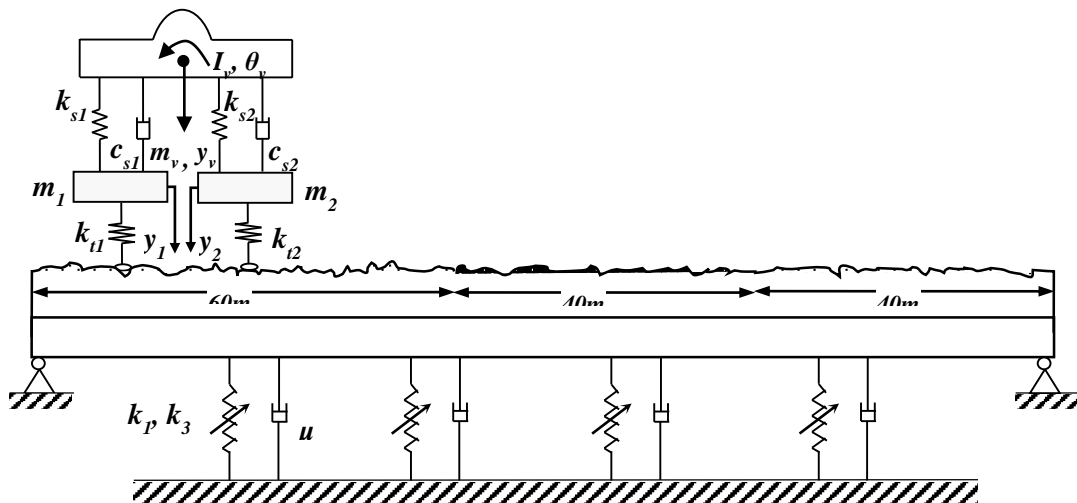


Fig. 5 Schematic representation of vehicle -pavement system

5. Results

The investigations are carried out, using Objective function J_1 for no measurement noise condition and 10% noise condition. When a limited number of parameters need to be estimated, with information at hand about the vehicle parameters is sufficient, J_1 could be utilized to full efficiency. The investigations are carried out using Objective function J_2 , for robust results in the cases of limited information. The effect on different vehicle speeds and roughness classes are also studied. Results of roughness estimates along with the vehicle parameters and states are detailed in the following sections. Results prove the capability of the proposed technique to yield accurate and robust estimates.

5.1 Using objective function 1 (J_1)

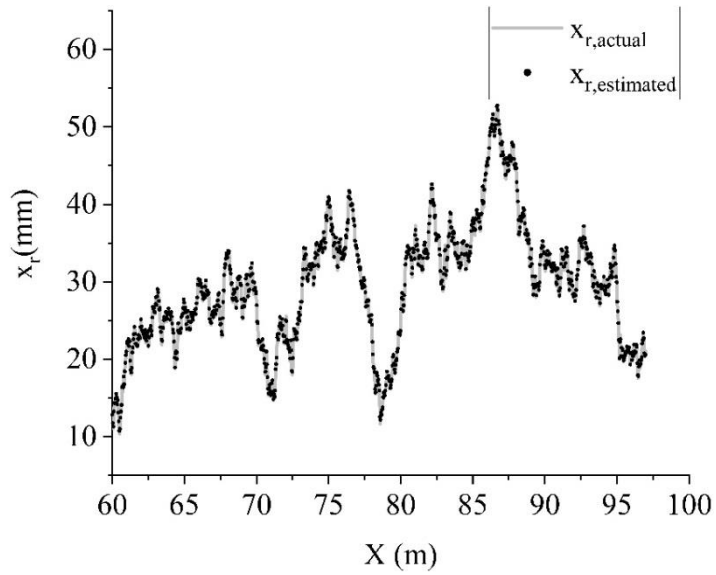
No measurement noise

Well-posedness of the optimization problem is a crucial element in determining the efficacy of the estimation, using the adopted technique. Initially, no noise measurement data condition is tested to check for the ill-posedness of the problem. Starting with the case of the number of unknown vehicle parameters equals one, it has been found that up to five parameters can be estimated effectively, with less than 1% error as shown in Table 5. Different combinations of vehicle parameters are studied and found that the combinations involving tire stiffnesses (k_{t1} and k_{t2}) are prone to higher errors, indicating the problem is ill-posed, without a unique solution. Tire weights (m_1 and m_2) are easy to measure at the site and hence, kept known in all the numerical experiments in the present study.

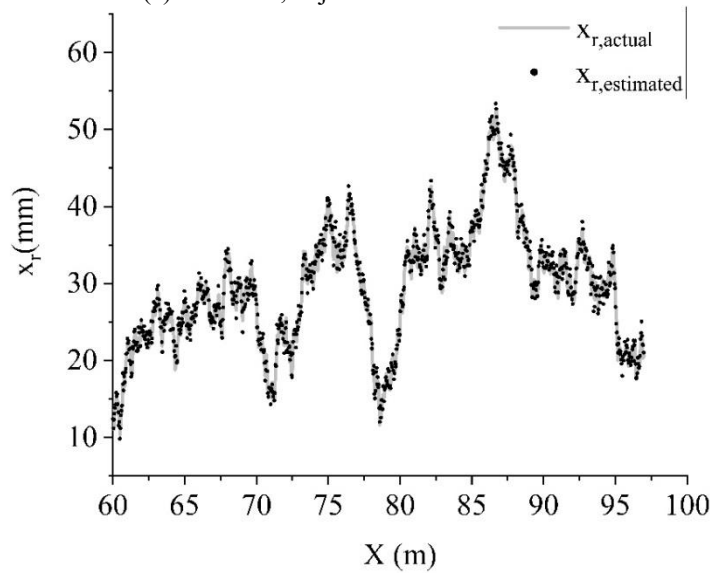
While keeping a maximum of five vehicle parameters as unknowns, the identification problem remains well-posed. Hence, for a number of unknown vehicle parameters up to five, the roughness can be estimated accurately. Fig. 6(a) shows the estimated average roughness profile is comparable with the actual field roughness profile. Roughness profiles are estimated at both rear and front wheel points and averaged to get a final estimate of roughness. Roughness estimate has a root mean squared error (RMSE) of $1.3 \times 10^{-4}m$. Effect of interaction on the roughness profile is assumed to be negligible throughout the study. It may be taken into account via a post-processing stage for better results.

With Measurement noise

After finding five parameter estimation problem as a well-posed problem, the whole procedure is tested on noisy measurement data, to check for the robustness of the results. For this test set, tire stiffnesses, tire masses, and ks_2 are kept known. From the observation that the objective function minimization results will improve for a lower percentage noise in the measurements, noisy measurements that are fed into the objective function pre-filtered. The displacements $[x_v, x_\theta]$ are smooth functions, and so, pre-filtering scheme chosen is Gaussian moving Average filter. The window size adopted is 50, for filtering. Estimation errors for vehicle parameters are as in Table 6 and are observed to be within acceptable limits. Roughness profile comparison is as shown in Fig. 6(b) and estimates are found to be comparable with actual profile and reasonably accurate. RMSE in this case is calculated as $8.3 \times 10^{-4} m$. As mentioned in no noise case, consideration of interaction may improve accuracy, though not necessary.



(a) No Noise, objective function 1



(b) 10% Noise, objective function 1

Fig. 6 Estimated Vs Actual Roughness Profiles

Table 5 Percentage error in parameter estimates with objective function J_1 (no measurement noise)

Physical constants	% error				
M_v	0.32	0.20	0.11	0.10	0.16
I_v	0.10	0.03	0.15	0.12	0.05
m_1	known	known	known	known	known
m_2	known	known	known	known	known
k_{s1}	0.13	known	0.10	0.10	0.03
c_{s1}	0.19	0.06	known	0.12	known
k_{s2}	known	0.11	0.17	0.22	0.15
c_{s2}	0.25	0.13	0.07	known	known
k_{t1}	known	known	known	known	known
k_{t2}	known	known	known	known	6.94

Table 6 Estimation errors

Vehicle Parameters	M_v	I_v	k_{s1}	c_{s1}	c_{s2}
Error %	1.4	0.93	0.03	0.92	1.67

5.2 Using objective function 2 (J_2)

The objective function J_1 handles an identification problem consisting of only up to 5 parameters along with roughness and states. Further improvement in the roughness estimates can be achieved if a higher number of parameters can be estimated simultaneously with roughness and states. The objective here is estimating up to 8 vehicle parameters which exclude tire masses which can be easily measurable. Numerical experiments are carried out with no noise measurements and 10% noise measurements. Additional information for the second term in the objective function J_2 requires the estimation of the natural frequency of the vehicle from the field measurement data.

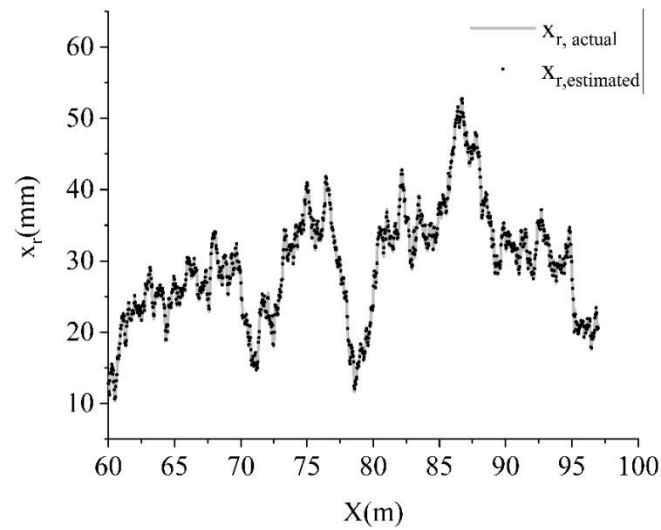
Natural frequency estimation

The acceleration responses ($\ddot{x}_v, \ddot{x}_\theta, \ddot{x}_{w1}, \ddot{x}_{w2}$) of the half car model recorded on the full 160 m length stretch of pavement is processed through Fast Fourier Transform, with a 5 % noise consideration in data records. The analysis of the peaks yields the frequencies as [1.163 Hz, 2.28 Hz, 10.21 Hz, 14.8 Hz]. This set of values forms the regularization equivalent term of objective function 2.

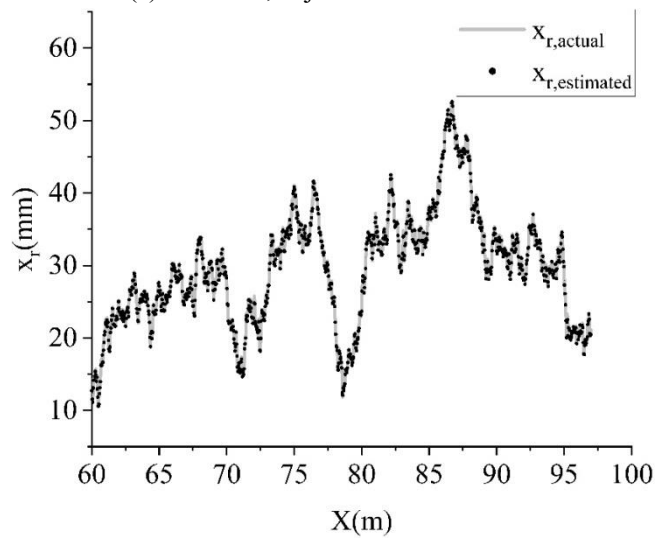
No measurement noise

The results from optimizing the objective function J_2 indicate the well-posedness of the eight parameter identification formulation. Estimated values with errors are listed in Table 7. The roughness profile is shown in comparison with the actual profile in Fig. 7(a). The two profiles are found to be comparable. It may be noted that simultaneous estimation of vehicle parameters even

in an increased number of eight parameters, with roughness and states, are feasible with Objective function J_2 . Moreover, the roughness estimates are maintaining reasonable accuracy, with an RMSE value of 1.6×10^{-4} .

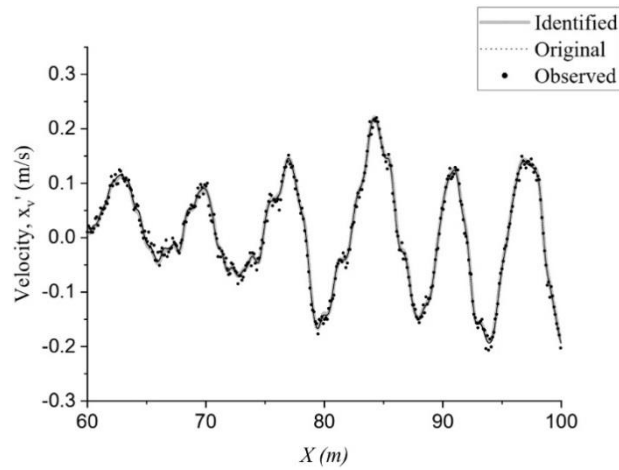


(a) No Noise, objective function 2

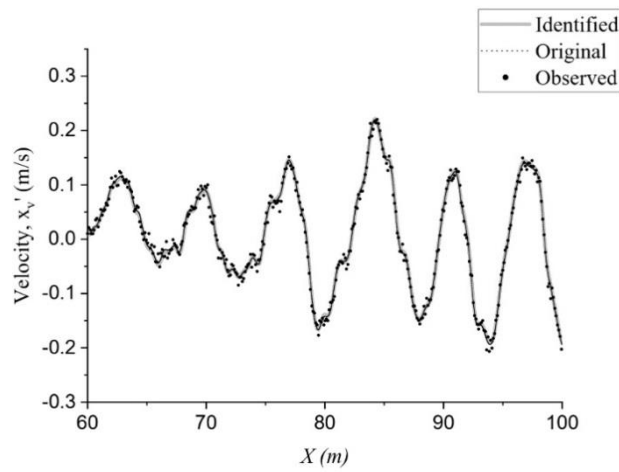


(b) 10% Noise, objective function 2

Fig. 7 Estimated Vs Actual Roughness Profiles



(a) Objective function 1



(b) Objective function 2

Fig. 8 Estimated Vs Actual States, Vehicle velocity \dot{x}_v

With Measurement noise

Observation data with 10% noise is fed into the framework, and minimization of Objective function yields an accurate estimate of vehicle parameters, and thereby, that of roughness and states. A sample set of results is listed in Table 7, and the roughness profile estimated as an average of that at rear and front wheels is shown in comparison with the actual profile in Fig. 7(b). The profiles are well comparable as mentioned and the estimate has an RMSE value of 1.6×10^{-4} .

Table 7 Percentage error in parameter estimates with Objective function J_2

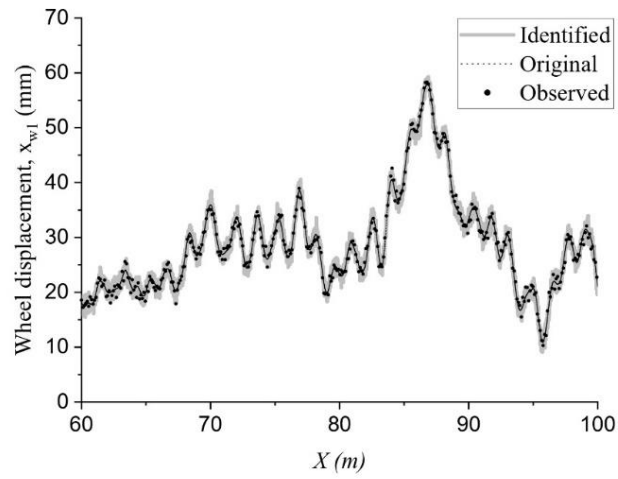
Physical parameter	No measurement noise		10% measurement noise	
	Estimated values	% error	Estimated values	% error
M_v	17767	0.18	17772	0.21
I_v	1.47×10^5	0.17	1.47×10^5	0.15
k_{s1}	2.48×10^6	0.22	2.50×10^6	0.88
c_{s1}	2.99×10^4	0.32	3.02×10^4	0.62
k_{s2}	4.13×10^6	2.46	4.32×10^6	2.17
c_{s2}	4.06×10^5	1.51	4.22×10^5	5.52
k_{t1}	3.74×10^6	0.10	3.72×10^6	0.65
k_{t2}	4.71×10^6	2.44	4.50×10^6	2.13

5.3 Filtered states

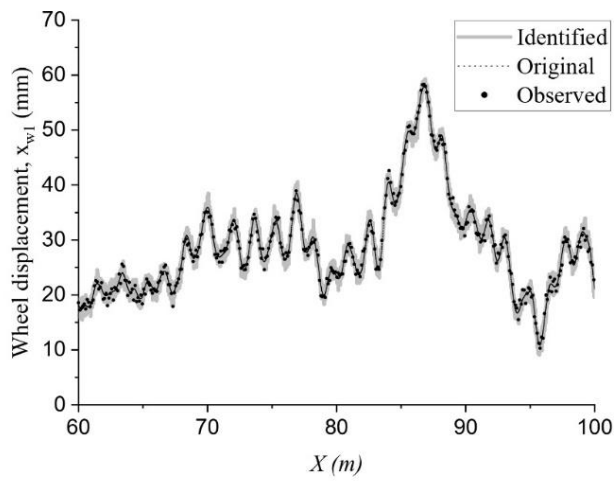
States are simultaneously estimated along with roughness and parameters for each of the cases discussed. The vertical vehicle velocity estimated for objective function J_1 and objective function J_2 are as shown in Figs. 8(a) and 8(b). The front wheel displacement estimated for objective function J_1 and objective function J_2 are as shown in Figs. 9(a) and 9(b). Their comparability with the actual responses reinforces the accuracy of the roughness estimates, towards the potential applicability as a deterioration indicator.

5.4 Variation with different road classes

Class B and Class C roughness profiles are generated in accordance with ISO 8608, based on power spectral density of road roughness. Entire procedure as for Class A is carried out, to simulate the results for the respective road classes. The comparative study considers the 8 parameter identification case with synthetic measurement data with an additive 10% noise and at vehicle speed of 5 m/s. The study considers the Objective function J_2 . The vehicle parameters and the roughness profiles are estimated, using the proposed technique. A comparative study on roughness estimation is shown in Fig. 10. The root mean square errors are calculated for each roughness class estimates and the variation is plotted in Fig. 10(d). The error is found to be of the order of 10^{-4} m. It is observed that though the estimation error increases with increase in the degree of roughness, the difference between errors is negligible. The vehicle parameter estimates for respective roughness classes are as enlisted in Table 8. The percentage errors based on the actual values are also listed. The parameter k_{s1} is found to have a relatively higher error, for Class B profile, still less than 10%. All other error values are found to be reasonably small.



(a) Objective function 1

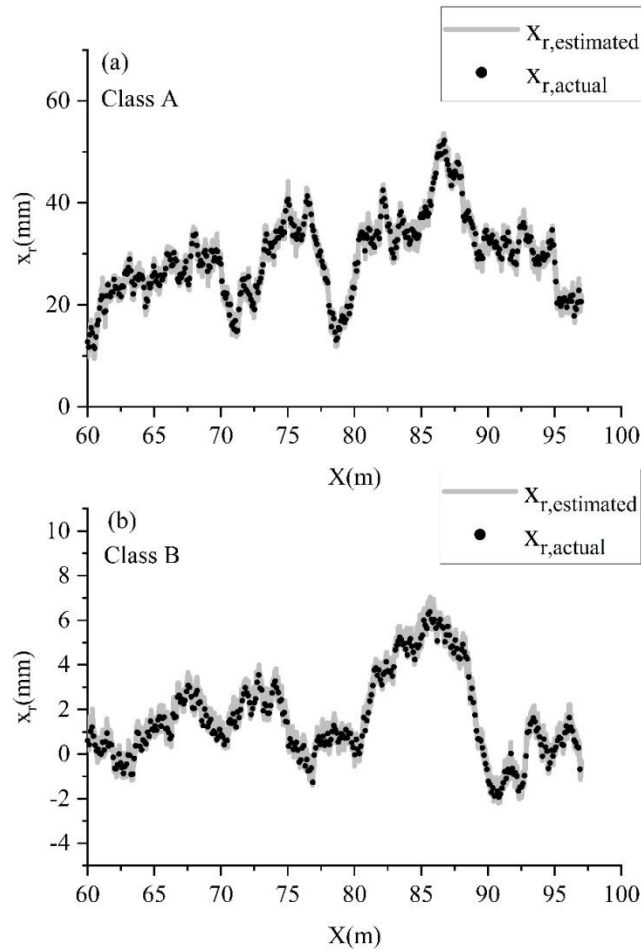


(b) Objective function 2

Fig. 9 Estimated Vs actual States, Front wheel velocity \dot{x}_{w1}

Table 8 Percentage error in parameter estimates with Objective function J_2 , for different roughness classes

Physical parameter	Class B		Class C	
	Estimated values	% error	Estimated values	% error
M_v	17650	0.48	17701	0.19
I_v	1.47×10^5	0.28	1.47×10^5	0.26
k_{s1}	2.42×10^6	2.06	2.47×10^6	0.08
c_{s1}	2.74×10^4	8.63	2.92×10^4	2.65
k_{s2}	4.25×10^6	0.36	4.35×10^6	2.81
c_{s2}	4.07×10^5	1.86	3.82×10^5	4.53
k_{t1}	3.80×10^6	1.48	3.74×10^6	0.01
k_{t2}	4.58×10^6	0.42	4.47×10^6	2.75



Continued-

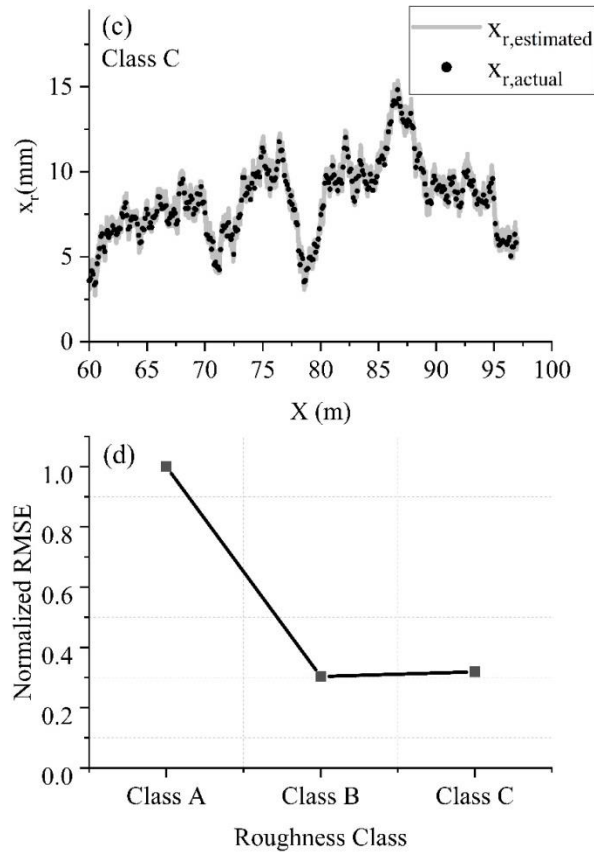
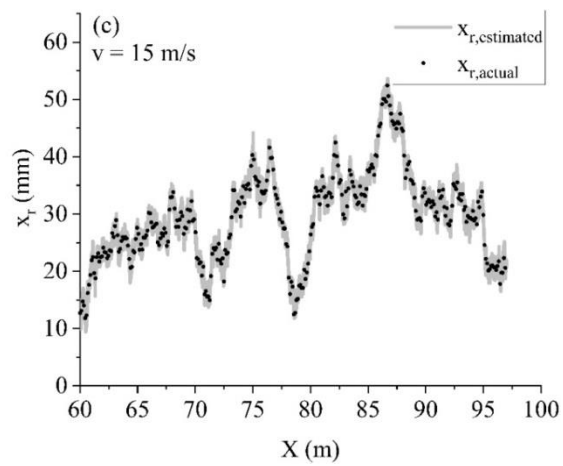
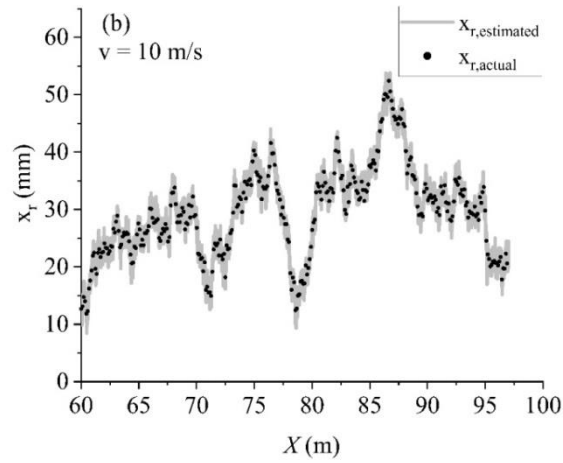
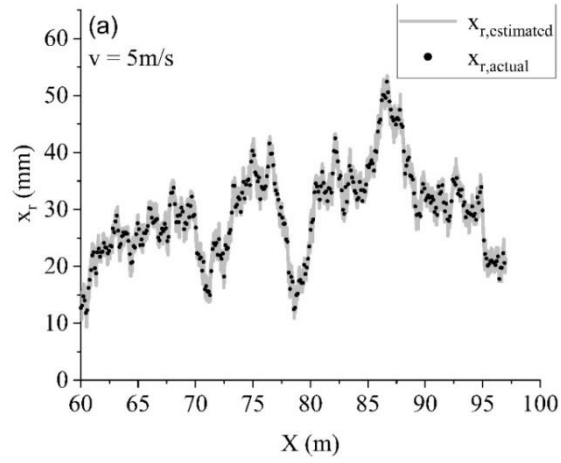


Fig. 10 Estimated Vs actual roughness for different road roughness classes and Normalised RMSE (a) For Class A (b) For Class B (c) For Class C (d) Normalised RMSE

5.5 Variation with different vehicle speeds

The study considers Class A roughness profile, measurement data with 10% noise and at vehicle speeds 5 m/s, 10 m/s, 15 m/s, 20 m/s and 25 m/s. The study considers the objective function J_2 . The roughness profiles are identified, considering the vehicle moving at different speeds. Roughness estimates are shown in Fig. 11 for each of the speed values and can be found comparable against the actual roughness profile. For further clarity regarding the accuracy, the root mean square errors (RMSE) are calculated with respect to the actual roughness profiles and found to be of the order of 10^{-3} and 10^{-4} m. Maximum error value obtained for speed 25 m/s and is 1.1×10^{-3} m. The normalized RMSE values are plotted in Fig. 11. A summary of percentage errors for the estimated vehicle parameters are shown in Fig. 12. The errors are found to be well within a reasonable limit (say 10%).



Continued-

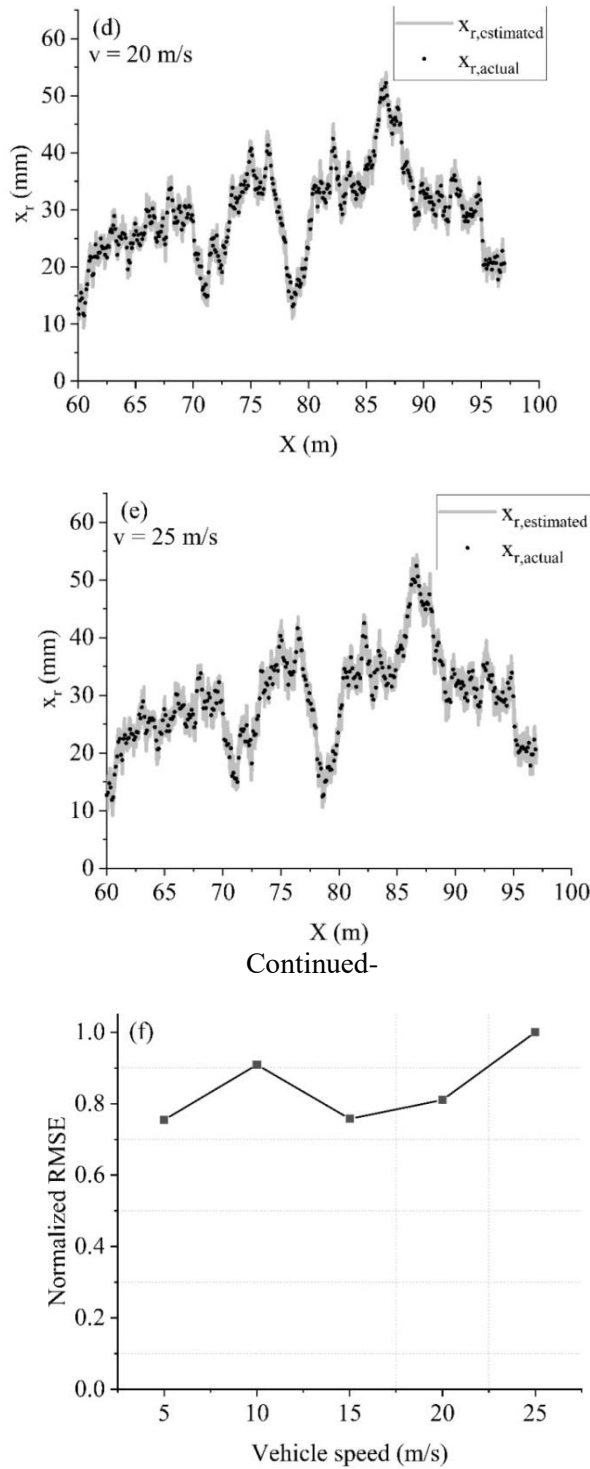


Fig. 11 Estimated Vs actual roughness for different vehicle speeds, v and the normalised RMSE (a) For $v = 5$ m/s (b) For $v = 10$ m/s (c) For $v = 15$ m/s (d) For $v = 20$ m/s (e) For $v = 25$ m/s (f) Normalized RMSE

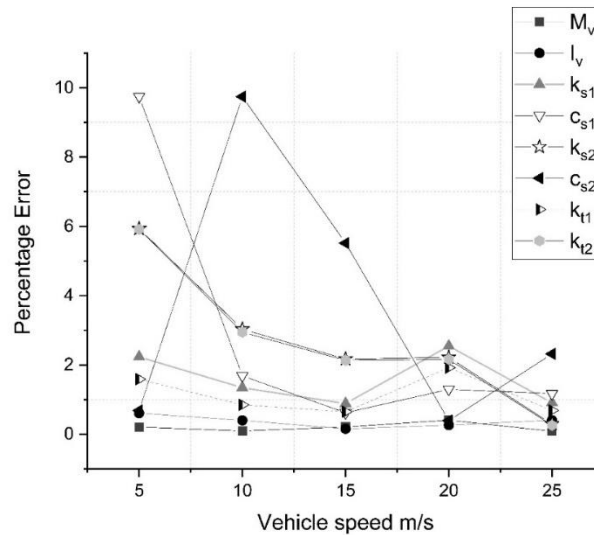


Fig. 12 Percentage errors of estimated vehicle parameters for different vehicle speeds

6. Conclusions

Roughness profile is identified accurately, with a robust scheme which combines MVE and an optimization scheme. The accuracy and robustness of the results indicate the potential use of the technique in the condition assessment of pavements. The study explores the use of two objective functions in the method, for the problem considered, at various vehicle speeds and roughness classes.

Major conclusions are as follows:

(i) The vehicle-road coupled system model consists of a half car vehicle model moving over a two-layer Euler–Bernoulli beam resting on a nonlinear Pasternak foundation (Snehasagar *et al.* (2019)), in this study. Use of the pavement foundation model, which incorporates viscoelastic behaviour leads to good results in the identification problem.

(ii) Objective function J_1 can be used for the estimation of parameters up to 5. When a limited number of parameters are only needed to be estimated, and others are accurately known, the proposed scheme with the objective function J_1 will be effective. Tire stiffness may yield relatively higher errors, but still within acceptable limits.

(iii) Objective function J_2 is efficient for estimating up to 8 parameters. While most of the parameters are uncertain, the objective function needs to be modified with the inclusion of an additional frequency term, which acts as a regularization parameter for the problem. Estimation errors are within acceptable limits.

(iv) Roughness estimates for no-noise condition, for five parameter identification problem, has an RMSE of 1.3×10^{-4} and for eight parameter identification problem has an RMSE of 1.6×10^{-4} . Errors are within the acceptable limits and found to be comparable.

(v) Roughness estimates for 10% noise condition, for 5 parameter identification problem has an RMSE of 8.3×10^{-4} and for 8 parameter identification problem has an RMSE of 8.3×10^{-4} . Errors are within the acceptable limits and found to be comparable. i.e., The technique gives accurate and stable estimates even when the observed data is corrupted with a higher percentage of noise.

(vi) The robustness of the estimation results are tested by varying the vehicle speeds and by varying the roughness classes, at a 10% noise measurement data, for eight parameter identification problem. Estimation errors (RMSE) of roughness profiles are of the order of $10^{-4} m$, for different road classes. While considering the accuracy over different vehicle speeds, RMSE is found to be of the order of $10^{-3} m$ and $10^{-4} m$. The error values are found to be small. Percentage errors of estimated vehicle parameters are below 10% and are within acceptable limits. Relatively higher errors are observed in the estimates of either of the damping parameters, at slower vehicle speeds and at any roughness condition.

(vii) Interaction effects may be accounted for, through a post-processing section. This study has not considered post-processing as good results are achieved even without a post-processing stage. The proposed technique offers the flexibility of using suitable and favourable models by the engineers or the designers as per the requirement, along with the algorithm, for better, practically efficient designs.

(viii) The comparability of the estimates with the actual solutions (states, vehicle parameters, and roughness) indicates the efficiency of the proposed technique. The procedure is not tested here against actual field data. With the foundation model, which provided comparable deflections with field observations, the technique is supposed to perform well with an actual data set.

References

- Agostinacchio, M., Ciampa, D. and Olita, S. (2014), "The vibrations induced by surface irregularities in road pavements—a Matlab® approach", *Eur. T. Res.Rev.*, **6**(3), 267.
- Alhasan, A., White, D.J. and De Brabanter, K. (2017), "Spatial pavement roughness from stationary laser scanning", *Int. J. Pavement Eng.*, **18**(1), 83-96.
- Au, F.T.K., Jiang, R.J. and Cheung, Y.K. (2004), "Parameter identification of vehicles moving on continuous bridges", *J. Sound Vib.*, **269**(1-2), 91-111.
- Chen, T.C. and Lee, M.H. (2008), "Research on moving force estimation of the bridge structure using the adaptive input estimation method", *J. Struct. Eng.*, **8**, 20-208.
- Ding, H., Yang, Y., Chen, L.Q. and Yang, S.P. (2014), "Vibration of vehicle pavement coupled system based on a timoshenko beam on a nonlinear foundation", *J.Sound Vib.*, **333**(24), 6623-6636.
- Fauriat, W., Mattrand, C., Gayton, N., Beakou, A. and Cembrzynski, T. (2016), "Estimation of road profile variability from measured vehicle responses", *Vehicle Syst. Dyn.*, **54**(5), 585-605.
- Gillespie, T.D. and Sayers, M.W. (1985), "Measuring Road Roughness and its Effects on User Cost and Comfort: A Symposium", *ASTM Int.*, **884**.
- Gillespie, T.D., Karamihas, S.M., Cebon, D., Sayers, M.W., Nasim, M.A., Hansen, W. and Ehsan, N. (2004), "Effects of heavy vehicle characteristics on pavement response and performance", University of Michigan Transportation Research Institute, UMTRI-92-2.
- Gillijns, S. and DeMoor, B. (2007), "Unbiased minimum-variance input and state estimation for linear

- discrete time systems”, *Automatica*, **43**(1), 111-116.
- Green F. and Cebon D. (1994), “Dynamic responses of highway bridges to heavy vehicle loads”, *J. Sound Vib.*, **170**, 51-78.
- González, A., O’Brien, E.J., Li, Y.Y. and Cashell, K. (2008), “The use of vehicle acceleration measurements to estimate road roughness”, *Vehicle Syst. Dyn.*, **46**(6), 483-499.
- Haddar, M., Baslamisli, S.C., Chaari, R., Chaari, F. and Haddar, M. (2018), “Road profile identification with an algebraic estimator”, *Proceedings of the Institution of Mechanical Engineers, Part C: Journal of Mechanical Engineering Science*, SAGE Publications Sage UK: London, England.
- Harris, N.K., González, A., O’Brien, E.J. and McGetrick, P. (2010), “Characterisation of pavement profile heights using accelerometer readings and a combinatorial optimisation technique”, *J. Sound Vib.*, **329**(5), 497-508.
- Hoshiya, M. and Maruyama, O. (1987), “Identification of running load and beam system”, *J. Eng. Mech.*, **113**(6), 813-824.
- Krishnanunni, C.G., Raj, R.S., Nandan, D., Midhun, C.K., Sajith, A.S. and Ameen, M. (2019), “Sensitivity based damage detection algorithm for structures using vibration data”, *J. Civil Struct. Health Monit.*, **9**(1), 137-151.
- Krishnanunni, C.G. and Rao, B.N. (2019), “Decoupled technique for dynamic response of vehicle-pavement systems”, *Eng. Struct.*, **191**, 264-279.
- Lalthlamuana, R. and Talukdar, S. (2015), “Obtaining vehicle parameters from bridge dynamic response: a combined semi-analytical and particle filtering approach”, *J. Modern T.*, **23**(1), 50-66.
- Law, S.S., Bu, J.Q., Zhu, X.Q. and Chan, S.L. (2004), “Vehicle axle loads identification using finite element method”, *Eng. Struct.*, **26**(8), 1143-1153.
- Li, S., Yang, S. and Chen, L. (2016), “Investigation on cornering brake stability of a heavy-duty vehicle based on a nonlinear three-directional coupled model”, *Appl. Math. Model.*, **40**(13-14), 6310-6323.
- Loizos, A. (2001), “A simplified application of fuzzy set theory for the evaluation of pavement roughness”, *Road & T. Res.*, **10**(4), 21.
- Loizos, A. and Plati, C. (2002), “Road roughness measured by profilograph in relation to user’s perception and the need for repair: A case study”, *International Conference on Pavement Evaluation*.
- Lyons, R.G. (2004), *Understanding digital signal processing*, 3rd edition, Pearson Education India.
- Mejlun, L., Judycki, J. and Dolzycki B. (2017), “Comparison of elastic and viscoelastic analysis of asphalt pavement at high temperature”, *Procedia Eng.*, **172**, 746-753.
- Sayers, M.W. and Karamihas, S.M. (1996), “Interpretation of road profile roughness data”, *University of Michigan Transportation Research Institute*, UMTRI-96-19.
- Sayers, M.W. and Karamihas, S.M. (1998), *The Little Book of Profiling*, University of Michigan Transportation Research Institute.
- Snehasagar, G., Krishnanunni, C.G. and Rao, B.N. (2019), “Dynamics of vehicle-pavement system based on a viscoelastic Euler-Bernoulli beam model”, *Int. J. Pavement Eng.*, 1-14.
- Yang, S., Li, S. and Lu, Y. (2010), “Investigation on dynamical interaction between a heavy vehicle and road pavement”, *Vehicle Syst. Dyn.*, **48**(8), 923-944.
- Yang, X.S. and Deb, S. (2009), “Cuckoo search via Lévy flights”, *Proceedings of the 2009 World Congress on Nature & Biologically Inspired Computing (NaBIC)*. IEEE.
- Yang, S., Chen, L. and Li, S. (2015), *Dynamics of vehicle-road coupled system*, Springer.
- Wang, H., Nagayama, T., Zhao, B. and Su, D. (2017), “Identification of moving vehicle parameters using bridge responses and estimated bridge pavement roughness”, *Eng. Struct.*, **153**, 57-70.
- Wei, W., Shaoyi, B., Lanchun, Z., Yongzhi, W. and Hui, Y. (2015), “1803. Pavement roughness identification research in time domain based on neural network”, *J. Vibroeng.*, **17**(7).
- Wu, S.Q. and Law, S.S. (2011), “Vehicle axle load identification on bridge deck with irregular road surface profile”, *Eng. Struct.*, **33**(2), 591-601.